fitness values for all the existing individuals is then calculated from:

$$S_{\rho-1} = \sum_{q=0}^{M-1} F_{\rho-1}(q) \quad (3)$$

The mutation point and the crossover point are selected randomly. This procedure is repeated until the maximum population size is searched.

Step 4: If the number of generation is less than the maximum number of generations, the process returns to step 1. After the maximum number of generations, the best chromosome is selected and represents the best channel allocation for the specified conditions.

Results: In an example of the simulation, a proposed S-UMTS configuration is chosen with 10 satellites that are distributed into two planes with five satellites for each plane. The altitude of satellites is 10355 km. The update interval time is chosen as 15 min and the sampling time as 1 min.

Experiment 1: We evaluate the traffic capacity per channel for 61, 36 and 19 spotbeams per satellite, respectively. The genetic engine works with 150 of the population size and 350 of the maximum number of generation. The mutation probability is chosen to be 0.01 and the crossover probability is 0.6 as suggested in [4]. The results of the traffic carried per channel for the genetic DCA and the conventional DCA for the whole service area assuming a blocking probability of 3% are summarised in Table 1. From these results, it can be seen that the genetic DCA outperforms the conventional DCA. The traffic capacity obtained using the genetic DCA is 1.23, 1.3 and 1.2 times that of the conventional DCA algorithm for 61, 36 and 19 spotbeams, respectively. In addition, the genetic DCA strategy is much more adaptable under conditions of high traffic intensity.

Experiment 2: We evaluate the call blocking probability for a mean request of 275 calls and 61 spotbeams per satellite, respectively. The maximum number of generation is chosen to be 500 with 0.01 as the mutation probability and 0.6 as the crossover probability. In this experiment, the population size of the genetic DCA is chosen as 50 and 150. The performances of the call blocking probability for the genetic DCA and the conventional DCA are shown in Fig. 2. The results show that the call blocking probability of the genetic DCA model tends to decrease more rapidly as the offered traffic intensity decreases and the population size increases.

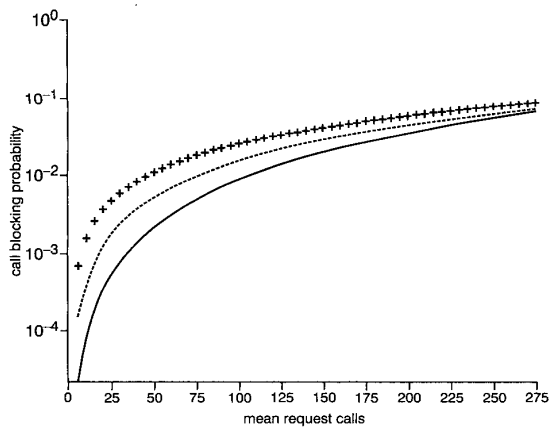

Fig. 2 *Call blocking probability*
———— GDCA with 150 population size
---------- GDCA with 50 population size
+ + + + conventional DCA

Table 1: Traffic carried per channel (Erlang/channel)

Channel allocation model	61 spotbeams	36 spotbeams	19 spotbeams
DCA	4.86	3.21	2.98
Genetic DCA	5.98	4.18	3.59

Conclusions: A new genetic DCA for MSS system networks has been proposed and evaluated. The results show that, using the new algorithm, the traffic carried per channel and the call blocking probability performance can be improved compared with the conventional DCA scheme. The new algorithm has been shown to be robust to dynamic variations and will provide resource allocation improvements in DCA in MSS system networks.

6 August 2002
Electronics Letters Online No: 20020844
DOI: 10.1049/el:20020844

M. Asvial, B.G. Evans and R. Tafazolli (*Centre for Communications Systems Research, University of Surrey, Guildford, GU2 7XH, United Kingdom*)

E-mail: a.muhamad@eim.surrey.ac.uk

References

1 DEL RE, E., FANTACCI, R., and GIAMBENE, G.: 'Handover queuing strategies with dynamic and fixed channel allocation techniques in low earth orbit mobile satellite systems', *IEEE Trans. Commun.*, 1999, **47**, (1), pp. 89–101
2 CHO, S.: 'Adaptive dynamic channel allocation scheme for spotbeam handover in LEO satellite networks'. Proc. of VTC 2000, Boston, MA, USA, September 2000, pp. 1925–1929
3 BECKMANN, D., and KILLAT, U.: 'A new strategy for application of genetic algorithms to the channel assignment problem', *IEEE Trans. Veh. Technol.*, 1999, **48**, (4), pp. 1261–1269
4 GOLDBERG, D.E.: 'Genetic algorithm in search, optimization, and machine learning' (Addison Wesley, 1989)

Experimental evaluation of unsupervised channel deconvolution for wireless multiple-transmitter/multiple-receiver systems

D. Samardzija, C. Papadias and R. Valenzuela

An over-the-air demonstration of unsupervised (blind) multiple-input/multiple output (MIMO) channel deconvolution is presented. The results were obtained in an indoor multiple antenna (BLAST) context. A suitable unsupervised MIMO technique was used in order to avoid the effective reduction of spectral efficiency caused by the use of channel training. To the authors' knowledge, this may be the first reported experiment of successful over-the-air unsupervised MIMO deconvolution.

Introduction: The Bell-labs LAyered Space-Time (BLAST) architecture [1] uses multiple antenna elements at both the transmitter and the receiver to provide high-capacity wireless communications in a rich scattering environment. The theoretical multiple-input/multiple output (MIMO) channel capacity increases roughly linearly with the number of *Tx*/*Rx* antennas [1].

Receiver algorithms typically require explicit knowledge of the MIMO channel response, which in turn requires the use of training or pilot sequences that limit the spectral efficiency of the system. To avoid the training overhead, unsupervised (blind) alternatives should be sought. A large number of so-called blind source separation (BSS) techniques for MIMO channels can be found in the literature [2]. In the work presented in this Letter, our goal has been to demonstrate over-the-air the applicability of such techniques to wireless BLAST-type systems.

Owing to their highly nonlinear objective functions, BSS techniques may often converge to false (undesired) solutions. For this reason, we have focused on a recently introduced technique [3], which was theoretically shown to be globally convergent to a setting that recovers all the input signals. The technique is called the multi-user kurtosis (MUK) algorithm and it is based on a deflation-type optimisation of a cost function that contains the output signals' fourth-order cumulants under second-order (whiteness) constraints.

For the purposes of this work, we used a MIMO narrowband wireless test bed that we have built for verification and performance evaluation of different algorithms related to BLAST architectures (see [4, 5]). In this Letter we use bit error rate (BER) as a performance metric, and we compare the MUK scheme against well-known trained solutions. As

shown in the following, our experimental results suggest the applicability of BSS techniques to real MIMO systems.

Baseband processing: The baseband received vector is modelled as

$$\mathbf{r}(k) = \mathbf{H}\mathbf{a}(k) + \mathbf{n}(k) \quad (1)$$

$\mathbf{H}$ is an $N \times M$ complex-entry matrix that corresponds to the narrowband MIMO channel response. $\mathbf{a}(k)$ is a complex input (data) $M \times 1$ vector and $\mathbf{n}(k)$ is the $N \times 1$ additive white Gaussian noise (AWGN) impairment, all corresponding to the kth time sample. To recover input vector $\mathbf{a}(k)$, $\mathbf{r}(k)$ is filtered by an $N \times M$ 'spatial equaliser' $\mathbf{W}$ which results in output vector $\mathbf{z}(k) = [z_1(k) \ldots z_M(k)]^T$ as

$$\mathbf{z}(k) = \mathbf{W}^T\mathbf{r}(k) = \mathbf{G}^T\mathbf{a}(k) + \mathbf{n}'(k) \quad (2)$$

$\mathbf{G}$ is the $M \times M$ global response matrix, $\mathbf{n}'(k) = \mathbf{W}^T\mathbf{n}(k)$ and T denotes transpose. The MUK algorithm [3] first updates $\mathbf{W}(k)$ in the direction of the MUK criterion's gradient as

$$\mathbf{W}'(k+1) = \mathbf{W}(k) - \mu\mathbf{r}^*(k)\mathbf{Z}(k) \quad (3)$$

where $\mathbf{Z}(k) = [|z_1(k)|^2 \ldots |z_M(k)|^2]^T$, and μ is a small step size. A Gram-Schmidt orthogonalisation of the columns of $\mathbf{W}'(k+1)$ is then performed, resulting in $\mathbf{W}(k+1)$ the columns of which are orthogonal (see [3]). Note that before the algorithm is run, the received signal $\mathbf{r}(k)$ needs to be pre-whitened (resulting in a unitary $\mathbf{H}$).

The MUK algorithm is executed on a data set which has L symbols, and corresponds to a frame which is communicated over the air. All the L symbols are information bearing, i.e. no portion of the frame is dedicated to a training sequence. To improve the results of the adaptation in (3), the above algorithm can be re-run several times using the same data set, i.e. the same frame, before the detection of the transmitted data is performed. For the particular implementation of the MUK algorithm in this Letter, we use $\mu = 0.04$. Also, we perform four re-runs to obtain the matrix $\mathbf{W}$.

Narrowband MTMR wireless test bed: The radio frequency (RF) front end of the test bed consists of an antenna array, and the corresponding array of analogue RF transmitters and receivers. The carrier is at 1.95 GHz and the signal bandwidth is limited to 30 KHz. The baseband digital signal processing is executed using a DSP multiprocessor system, Pentek 4285. It consists of eight Texas Instrument's TMS320C40 DSPs, offering a total processing power of 400MIPS. The interfacing towards the baseband is realised using a system of multichannel A/D (Pentek 4275) and D/A (Pentek 4253) converters, respectively. The maximum sampling rate per baseband channel is 100 KHz.

Experimental results: We present results that correspond to non-line-of-site indoor over-the-air trials. We use $M = 4$ transmit and $N = 6$ receive antennas and uncoded quaternary phase shift keying (QPSK) modulation on each antenna. The symbol frames are organised as follows. Symbols 1 to 16 are used for synchronisation, i.e. frame and symbol timing recovery (this part of the frame is identical for all sub-streams). K symbols compose a training sequence, which is used for estimation of the MIMO channel response (between the sub-streams, the sequences are mutually orthogonal and with equal transmit power). No training is used for the MUK, thus increasing its effective throughput.

For the trained receivers, we observe the performance for training lengths $K = 10$ and 20 symbols. The frame length is set to $L = 100$ or 200 symbols, i.e. 4 or 8 ms, respectively. The channel estimation is performed at the beginning of the frame, and no channel tracking is executed later, i.e. it is assumed that the channel is static during the frame period. This assumption is valid for indoor MIMO channels (mostly pedestrian speeds). The MUK adaptive algorithm uses all 100 or 200 symbols for the adaptation and, as stated earlier, it does not use a training sequence ($K_{muk} = 0$).

Fig. 1 shows the eye diagram per sub-stream after the fourth re-run of the MUK. We also present the squared error between z_p (output of the MUK algorithm for $L = 200$) and transmitted data a_p ($p = 1, \ldots, 4$), after the outputs are properly re-ordered. From the results we observe the ability of the MUK scheme to perform fully blind channel deconvolution and source separation. Fig. 2 shows the CDF of the BER estimate (measured per frame) obtained from our over-the-air indoor trials. Measured signal-to-noise ratio (SNR) is $\simeq 12$ dB. From the results, it is clear that the MUK algorithm does not fail during these real communication sessions. The trained receivers (linear minimum mean squared error (MMSE) and nonlinear V-BLAST [4]) do perform better at this SNR, but the MUK algorithm is able to follow the performance of the MMSE detector. Note that the MUK algorithm increases the throughput by 20% (for $L = 100$ and $K = 20$) and/or 10% (for $L = 100$ and $K = 10$), at the price of somewhat higher BER. We have also run the system for lower SNRs: both linear solutions (MUK and MMSE) outperformed the uncoded V-BLAST receiver at SNRs below 2 dB.

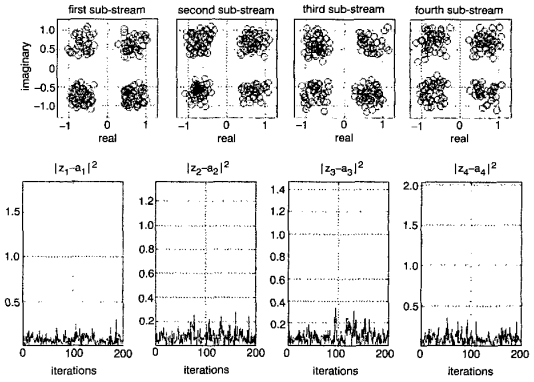

Fig. 1 *Eye diagram and squared error per sub-stream, after fourth re-run ($L = 200$, $M = 4$, $N = 6$, over-the-air trials, SNR~12 dB)*

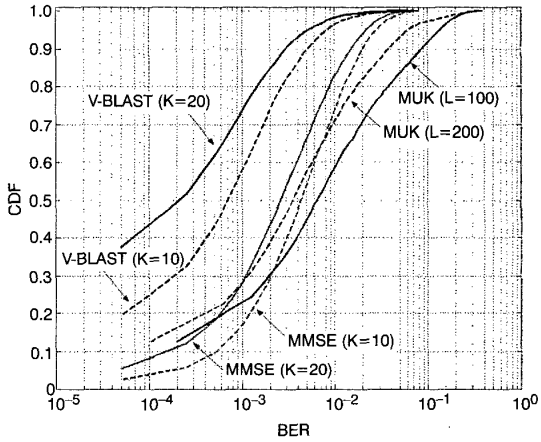

Fig. 2 *CDF of BER, $M = 4$, $N = 6$, over-the-air trials, SNR~12 dB*

Conclusion: We have validated the excellent performance of the MUK algorithm in an over-the-air wireless MIMO environment. Based on the results, we believe that blind approaches can be successfully used in true MIMO wireless systems.

12 July 2002
Electronics Letters Online No: 20020845
DOI: 10.1049/el:20020845

D. Samardzija, C. Papadias and R. Valenzuela (*Wireless Research Laboratory, Bell-Labs, Lucent Technologies, 791 Holmdel-Keyport Road, Holmdel, NJ 07733, USA*)

E-mail: dragan@lucent.com

References

1 FOSCHINI, G.J.: 'Layered space-time architecture for wireless communication in a fading environment when using multiple antennas', *Bell Labs Tech. J.*, 1996, **1**, (2), pp. 41–59

2 HAYKIN, S. (Ed.): 'Unsupervised adaptive filtering', Vols I and II (Wiley & Sons, Inc, 1999)

3 PAPADIAS, C.B.: 'Globally convergent blind source separation based on a multiuser kurtosis maximization criterion', *IEEE Trans. Signal Process.*, 2000, **48**, (12), pp. 3508–3519
4 GOLDEN, G.D., FOSCHINI, C.J., VALENZUELA, R.A., and WOLNIANSKY, P.W.: 'Detection algorithm and initial laboratory results using V-BLAST space-time communication architecture', *Electron. Lett.*, 1999, **35**, (1)
5 ZHENG, H., and SAMARDZIJA, D.: 'Performance evaluation of indoor wireless video system using BLAST test-bed'. CISS 2001, The Johns Hopkins University, Baltimore, 2001

Modified GSC for hybrid satellite constellation

M. Asvial, R. Tafazolli and B.G. Evans

A modified genetic satellite constellation (GSC) design is proposed for hybrid satellite constellations. The novelty of the proposed model is the automatic determination of satellite constellation parameters for hybrid LEO/MEO constellations. Illustrative results of satellite constellation parameters and dual satellite diversity statistics for hybrid LEO/MEO are presented.

Introduction: The genetic algorithm (GA) has been introduced as a robust technique to solve many multivariable problems [1]. Simulated annealing and genetic algorithms for satellite constellation design have been proposed to achieve the optimal discontinuous coverage and satellite constellation geometries in [2]. The discrete time step coverage in different designs providing the same value of maximum revisit time have been evaluated. Genetic satellite constellation (GSC) design for non-GEO inclined circular orbits with dual satellite diversity was additionally introduced in [3]. Here, GA for LEO and MEO constellation design is proposed to minimise the total number of satellites while minimising the maximum satellite's altitude. This algorithm is also applicable to optimise various parameters of the satellite constellation simultaneously.

In this Letter, a modified GSC is proposed for the design of hybrid satellite constellations with prescribed satellite diversity. The constellation chosen to demonstrate the technique is a hybrid LEO (lower layer) plus MEO (upper layer) constellation. The objective of the algorithm is to jointly optimise parameters of the constellation in both of the lower and the upper layers. The optimised parameters include the total number of satellites, the maximum satellite's altitude, the angle shift between satellites, the angle between planes and the inclination angle.

Satellite constellation type: For the example, the constellation is assumed to be an inclined circular orbit where all satellites have the same inclination angle and altitude. Each orbit contains an equal number of satellites. This constellation is proposed as it offers high diversity global coverage with a trade-off between diversity and number of satellites or minimum elevation angle. The contiguous coverage for the same altitude is provided by the dynamic overlap between the satellites in different planes. The lower and upper layers of the satellite constellation are designed for a resonant orbit with repetitive ground track and also to avoid the Van Allen radiation belts.

Genetic algorithm: The parameters of the satellite constellation are represented as hybrid chromosome structures in the genetic algorithms process. The parameters include the number of satellites, the altitude of satellite's orbit, the angle between planes, the angle shift between satellites, and the inclination angle for both layers of satellite constellation. In simulation, the same length of each chromosome for each variable is applied. The individual is represented by the total chromosome length and used in further steps of the genetic algorithm, such as selection, crossover and mutation. The chromosome structure of the GA for hybrid satellite constellation design is shown in Fig. 1.

A fitness function for all parameters as an element of dual satellite diversity is evaluated for each generation. The interpolation between the best and the worst Pareto rank is then examined for each fitness value. The same weighting factor (ω) for all objective functions is determined to control the optimal solution. The fitness function of this algorithm can be expressed as:

$$F_j^l = \frac{1}{1 + \dfrac{\left|\omega \prod_{k=1}^{2} E_{\min_k}(s,h,\theta)\right|}{\left|\omega \prod_{k=1}^{2} E_{\max_k}(\varphi,i)\right|} \times a^{-1}} \qquad (s,h,\theta,\varphi,i) \in SatDiv \tag{1}$$

where j is the generation number, $l = 1, \ldots, N$ is the identification index for each individual, k is the number of layer for hybrid constellation, and a is the scaling factor. Satellite parameters for both LEOs and MEOs are represented as s, h, θ, φ and i for the number of satellites, the altitude of satellite, the angle shift between satellites, the angle between planes and the inclination angle. $E_{\min_k}(\cdot)$ and $E_{\max_k}(\cdot)$ are the expectation operators of parameters with minimising and maximising value. A different scaling factor is examined to increase the robustness of generation to map the fitness values in the range 0 and 1. All parameters retain the satellite diversity condition (*SatDiv*).

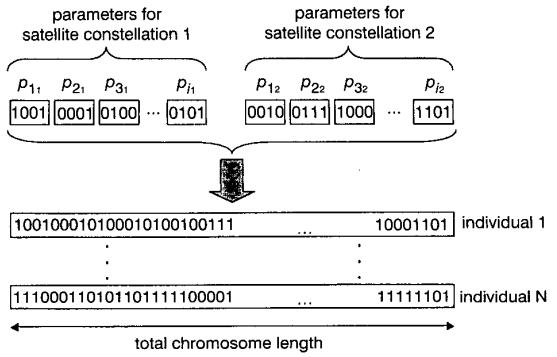

Fig. 1 *Chromosome structure*

The fitness of the two offspring individuals depends on the parents through the crossover and the mutation processes. The best fitness for each chromosome according to the satellite diversity for all parameters is then calculated. Multipoint crossover and non-uniform mutation processes are used in the algorithm. The best chromosome fitness can be written as:

$$chromosome\_fitness = \sum_{j=1}^{\max} F_j^l \tag{2}$$

The process is carried out on a group of the fittest individuals that represent all parameters of the satellite constellation. The chromosome matrix output of the genes of the satellite constellations can be written as:

$$c = [p_1^m, \ldots, p_1^n, p_2^m, \ldots, p_2^n,] \quad \text{for } m = (1, \ldots, n) \tag{3}$$

where p_{1or2}^m are the parameters of satellite constellations that are proposed in the GA. The genetic algorithm process can be stopped after an optimum number of generations. The best fitness is then chosen by ranking them from 1 to the maximum number of generations and thence stopping the process of selection, crossover and mutation.

Results: For the example genetic hybrid satellite constellation, population size is chosen as 350 with 550 of the maximum number of generation. The value of crossover probability and mutation probability are chosen as 0.6 and 0.025 as suggested in [1]. The constraint of the satellite's altitude parameter is chosen as 700–1700 km for LEO and 8000–17000 km for MEO.

In this simulation, dual satellite diversity is employed for both LEO and MEO orbits. Simulation results for the satellite parameters are shown in Table 1. The hybrid LEO and MEO constellation have 30 satellites for LEO (5 planes × 6 satellites per plane) and six satellites for MEO (2 planes × 3 satellites per plane). Compared to previous results [3], the number of satellites is seen to be reduced. Also the maximum satellite altitude for the hybrid constellation for both LEO and MEO are lower than for the single layer of satellite constellation presented in [3]. This will result in less delay and thus improved QoS for some services.